Thickness-dependent changes in the optical properties of PPV- and PF-based polymer light emitting diodes

J. M. Leger and S. A. Carter*
Physics Department, University of California, Santa Cruz, California 95064, USA

B. Ruhstaller†
IBM Zurich Research Laboratory, 8803 Rueschlikon, Switzerland

H.-G. Nothofer and U. Scherf‡
Institut für Physikalische und Theoretische Chemie, Universität Potsdam, D-14476 Golm, Germany

H. Tillman and H.-H. Hörhold‡
Institut für Organische und Makromolekulare Chemie, Friedrich-Schiller-Universität Jena, D-07743 Jena, Germany
(Received 13 February 2003; published 26 August 2003)

We explore the thickness-dependent optical properties of single layer polymer light emitting diodes for two materials, poly[2-methoxy-5-(2-ethylhexyloxy)-1,4-phenylene-ethenylene-2,5-dioctyloxy-1,4-phenylene-ethenylene] (MEH-DOO-PPV) and poly(2,7-(9,9-bis(2-ethylhexyl))fluorene)-2,7-bis(4-methylphenyl)phenylamine (PF with 2% endcap). We compare experimental electroluminescence spectra and radiance values as a function of emissive layer thickness with simulations utilizing dipole methods within a transfer-matrix formalism. The technique is then extended to explore how simulated results depend on the assumed location of emission within the polymer layer. We show that thickness-dependent optical properties of these devices are dominated by interference effects.

DOI: 10.1103/PhysRevB.68.054209 PACS number(s): 78.66.Qn

I. INTRODUCTION

Since the discovery of semiconducting polymers in 1990,[1] considerable progress has been made in understanding the electronic and optical properties of these materials in light emitting diode (LED) structures.[2] Our understanding, however, has been complicated by the fact that these properties can vary significantly for liquid processed polymer films[3] when the deposition conditions are varied. While there have been several studies on the effect of solvent and annealing conditions on the polymer film morphology,[4,5] few systematic studies have been done on understanding changes in the optical properties when varying the thickness in single layer devices.[6,7] This lack is surprising since modest changes in thickness in two of the more commonly studied class of materials, namely polyfluorenes and polyphenylenevinylenes, can result in substantial color shifts accompanied by order of magnitude changes in the device efficiency. Moreover, the polymer film thicknesses are frequently not reported or vary substantially, making comparisons between different experimental works difficult.

Thickness-dependent changes in the optical properties can be caused by changes in the self-absorption, local film morphology in the region of light emission, and optical interference (i.e., microcavity effects). In this paper, we explore the optical properties of single layer LED's as a function of emissive layer thickness in an attempt to understand the relative importance of these effects. Devices are made with poly[2-methoxy-5-(2-ethylhexyloxy)-1,4-phenylene-ethenylene-2,5-dioctyloxy-1,4-phenylene-ethenylene] (MEH-DOO-PPV) and with poly(2,7-(9,9-bis (2-ethylhexyl)fluorene)-2,7-bis(4-methylphenyl)phenylamine (PF with 2% endcap), materials that both show substantial changes in the CIE coordinates and device efficiency with thickness. The thickness-dependent properties of these devices are then compared with simulations that model the optical interference effects in single layer PLED structures. We find that this effect is the primary factor in understanding changes in the optical properties of our devices due to varying thickness.

II. EXPERIMENTAL METHODS AND RESULTS

The material synthesis and characterization of both MEH-DOO-PPV[8] and PF[9] have been described previously [for chemical structures see insets in Figs. 1(a) and (b)]. Polymer films were spin cast from solution on quartz substrates for absorption and photoluminescence measurements. Absorption spectra for PF and MEH-DOO-PPV films were measured using an n&k 1200 UV-VIS scanning spectrometer and a Hewlett-Packard 8452A Diode Array Spectrophotometer, respectively. Photoluminescence data were taken on a Perkin Elmer LS 50B luminescence spectrophotometer at absorption maximum. Normalized absorption and photoluminescence data are presented in Fig. 1, and showed minimal dependence on layer thickness.[10]

Devices were constructed using a single emissive layer structure with the addition of a hole transport layer. Poly(3,4,ethylenedioxythiophene)-poly(styrenesulfonate) (PEDOT-PSS)[11] of 60 nm thickness was spin coated onto patterned ITO on glass substrates and annealed at 128 °C for 1 h under vacuum.[12] The emitting polymer layer was spin coated from solution at various spin speeds and from solutions of varying concentrations to achieve a range of film

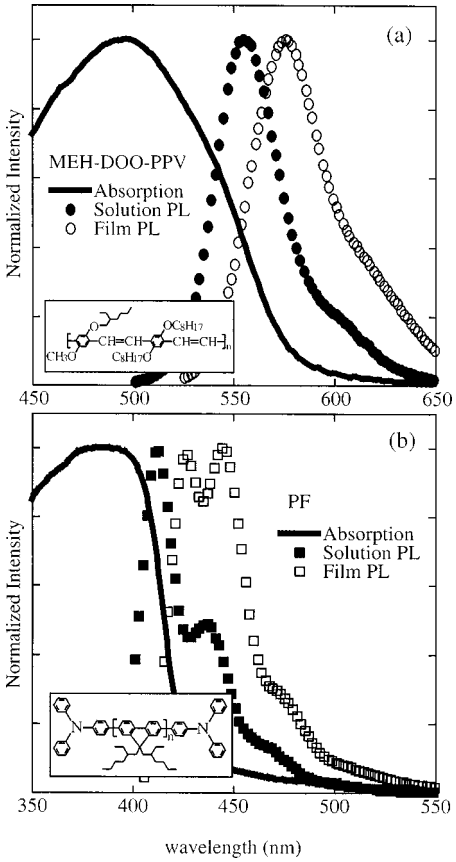

FIG. 1. Experimental normalized film absorption, solution PL, and film PL for (a) MEH-DOO-PPV and (b) PF. Inlays show the chemical structures for each polymer.

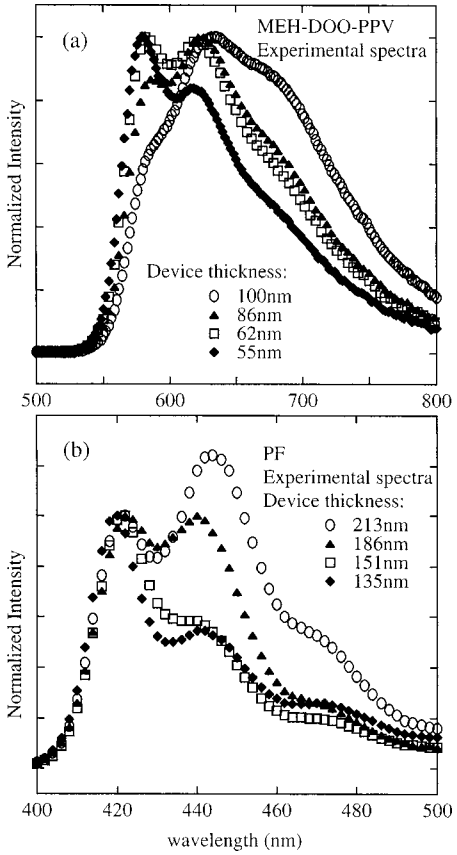

FIG. 2. Experimental normalized EL spectra for (a) MEH-DOO-PPV, with thicknesses 55, 62, 86, and 100 nm and (b) PF, with thicknesses 135, 151, 186, and 213 nm.

thicknesses. The MEH-DOO-PPV film thicknesses were varied between 55 and 100 nm, resulting in a color shift from orange (CIE 0.577, 0.422) to reddish (CIE 0.619, 0.379) emission. PF film thicknesses were varied between 135 and 213 nm, resulting in a color shift in this range from blue (CIE 0.191, 0.134) to violet (CIE 0.171, 0.092) emission. The error on measured layer thickness is ± 5 nm. The polymer layers are dried under vacuum overnight. A 25-nm layer of calcium followed by a 25-nm layer of aluminum is thermally evaporated onto the device. Thicknesses were measured on a Park Scientific Autoprobe CP Atomic Force Microscope (AFM). Current-voltage-radiance curves were taken in an inert nitrogen atmosphere with a Keithley source measure unit, a picoammeter, and a calibrated silicon photodetector. Electroluminescence spectra were also taken in an inert nitrogen atmosphere with an Ocean Optics fiber-optic spectrometer.

Figure 2(a) shows the normalized electroluminescence spectra from polymer LED's with MEH-DOO-PPV as the emissive material. Spectra are shown for polymer layer thicknesses of 55, 62, 86, and 100 nm. We observe a significant drop in the relative weight of the 580 nm vibrational peak and a concurrent rise in emission at lower energies as the thickness of the polymer layer is increased. The broad lower energy peak observed at ~680 nm may be attributed to aggregate emission.[13] Similarly, as shown in Fig. 2(b), the normalized electroluminescence spectra from polymer LED's with PF as the emissive material also show strong thickness dependence. Here, the spectra shown have thicknesses of 135, 151, 186, and 213 nm. Again we see a drop in the relative weight of the primary vibronic peak at 420 nm with increased emissive layer thickness.

III. SIMULATION THEORY

In order to understand the effects of optical interference on the properties of polymer LED's, we did simulations which model thickness dependence in single layer polymer LED structures. Since polymer LED's consist of a multilayer thin-film stack with a total thickness on the order of the emission wavelength, the emission spectra critically depend on the thicknesses and refractive indices of the individual layers. In the absence of a light source, one can write the solution to the one-dimensional Helmholtz equation $d^2\psi/dz^2+k^2\psi=0$ as the superposition of a right and left traveling plane wave $\psi=\psi^+e^{ikz}+\psi^-e^{-ikz}$. In layered media, the continuity conditions at layer boundaries can be written in matrix form.[14,15] For instance, the boundary transfer matrix relating the amplitudes ψ^+ and ψ^- of the adjacent layers l and $l+1$ for S polarization reads

$$\begin{pmatrix} \psi_l^+ \\ \psi_l^- \end{pmatrix} = \frac{1}{2} \begin{pmatrix} 1+\dfrac{k_{l+1}}{k_l} & 1-\dfrac{k_{l+1}}{k_l} \\ 1-\dfrac{k_{l+1}}{k_l} & 1+\dfrac{k_{l+1}}{k_l} \end{pmatrix} \begin{pmatrix} \psi_{l+1}^+ \\ \psi_{l+1}^- \end{pmatrix}, \qquad (1)$$

where the wave number $k=2\pi n/\lambda$ depends on the wavelength λ and the refractive index n, which becomes complex in the case of absorptive media. In addition, the propagation transfer matrix for plane-wave propagation in a layer of thickness Δz reads

$$\begin{pmatrix} \psi_l^+ \\ \psi_l^- \end{pmatrix} = \begin{pmatrix} \exp(jk\Delta z) & 0 \\ 0 & \exp(-jk\Delta z) \end{pmatrix} \begin{pmatrix} \psi_{l+1}^+ \\ \psi_{l+1}^- \end{pmatrix}. \quad (2)$$

Thus by multiplication of layer and boundary transfer matrices from multiple layers an effective matrix relating the wave amplitudes at different locations in the multilayer structure is obtained, from which the reflection and transmission Fresnel coefficients r and t are derived. For the simulation of light emission in a layered medium the inhomogeneous Helmholtz equation with a source consisting of an oscillating point dipole needs to be solved.[16–18] Dipole methods have previously been used successfully to model organic LED emission.[19,20] Such simulations in general require the distinction of parallel and vertical dipole orientations as well as S and P polarization. However, for emission in the normal direction the expression for the emitted power density simplifies to[18]

$$P \sim \frac{|1+r_l^- \exp(2ik_l z)|^2}{|1-r_l^- r_l^+ \exp(2ik_l d_l)|^2} \cdot |t_l^+|^2, \quad (3)$$

where r_l^+, r_l^-, and t_l^+ are the Fresnel coefficients for light originating in layer n, and z^- is the distance of the dipole from the lower boundary of layer n whose thickness is d_l. In expression (3) the denominator accounts for layer thickness-dependent multiple beam interference while the nominator depends on the dipole position within this layer.

IV. COMPARISON OF SIMULATION AND EXPERIMENT

For our investigations, we assume that the emission zone location scales with device thickness as expected if relative charge mobilities and injection rates remain unchanged. The simulation parameters thickness, refractive index, and basis spectra were determined experimentally. For both the PF and the MEH-DOO-PPV, we use an experimentally determined EL spectrum as the emission spectrum of the dipole. The refractive index dispersion curves of MEH-DOO-PPV and PF were determined by spectroscopic ellipsometry (VASE by Woollam Inc.). In particular, a Cauchy dispersion model was fit to the transparent regime and subsequent extrapolation to lower wavelengths was carried out by point-to-point fits. For this fit, an isotropic model was chosen, thus ignoring birefringence in the films. The model gives a very good fit to the experimental data. Inclusion of birefringence in the model is a subject of future work. The resulting dispersion curves are shown in Fig. 3. For PEDOT-PSS, a constant refractive index value of 1.53 was assumed.[21] The resulting simulated spectra are shown in Fig. 4(a) for the MEH-DOO-PPV emission and in Fig. 4(b) for the PF. We can see that in both the MEH-DOO-PPV and the PF simulations, for which we chose the same or similar thicknesses as our experimental devices, the simulations very closely match the experimentally determined spectra. We have shown that the simulations were successful in modeling the changes in the relative weights of the two leading vibronic peaks of the EL spectra with changing device thickness.

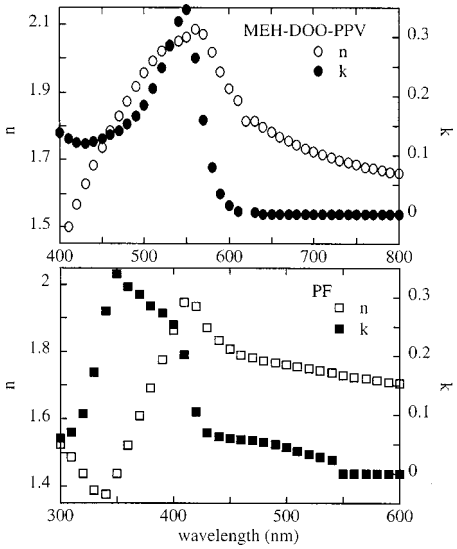

FIG. 3. Refractive index dispersion curves for MEH-DOO-PPV and PF.

In addition to simulating the EL spectra of these devices

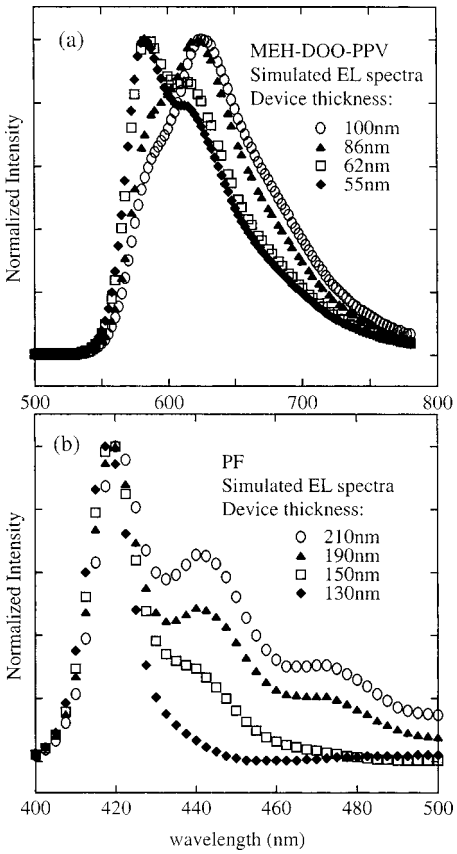

FIG. 4. Simulated normalized EL spectra for (a) MEH-DOO-PPV, with thicknesses 55, 62, 86, and 100 nm and (b) PF, with thicknesses 130, 150, 190, and 210 nm. Emission is assumed to occur 20% of device thickness away from the anode.

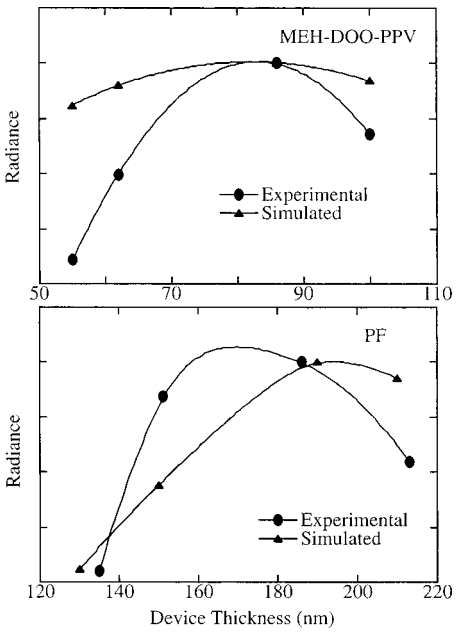

FIG. 5. Experimental and simulated radiance curves in arbitrary units, for (a) MEH-DOO-PPV and (b) PF. For the simulated results, emission is assumed to occur 20% of device thickness away from the anode.

as a function of device thickness, we looked at the radiance as a function of device thickness and compared the experimental data to the simulated results. Those results are plotted as Figs. 5(a) and (b). Experimentally determined values for radiance were measured at the same current for all devices. Values plotted in Fig. 5 were normalized to compare the relative changes in radiance with simulated results. The overall trends in relative radiance with device thickness are nicely reproduced in the simulated data.

We would expect that the trend in radiance with increased self-absorption would be a steady decrease with increasing device thickness, and so we can conclude that the observed trend in radiance is dominated by optical interference effects. In addition, self-absorption should have the effect of decreasing the relative intensity of the EL at wavelengths in the region of overlap between emission and absorption as the thickness of the polymer layer is increased. As seen in Fig. 1, this region is in both cases the leading vibronic peak in EL spectrum. Therefore the thickness dependent effects seen in the experimental EL spectra are at least partially due to self-absorption effects. However, the overlap is not large, and the difference in device thickness is not significant enough to completely explain the strong thickness dependence seen in the spectra of these devices. Again therefore we expect that interference may play the dominant role.

V. SIMULATION OF EMISSION ZONE LOCATION

For both the PF and the MEH-DOO-PPV thickness dependence simulations discussed above, we assumed the emission zone to be a distance 20% of the emissive layer thickness away from the anode. To come to this assumption, it was necessary to explore the dependence of the simulations on location of light emission. These simulations are shown in Figs. 6 and 7. First we explore several emission zone locations for a given device thickness in Fig. 6. Figure 6(a) shows a simulated 100 nm thick MEH-DOO-PPV device, with light emission occurring at various locations in the polymer layer. As the emission moves from the anode to the cathode, we see an increase in the first peak intensity as well as a slight blueshift in peak location. In contrast, the dependence on emission zone location for PF, shown in Fig. 6(b) for a 190 nm thick device, does not display a clear trend. We see that the emitted spectra for PF are highly sensitive to modest changes in emission zone location.

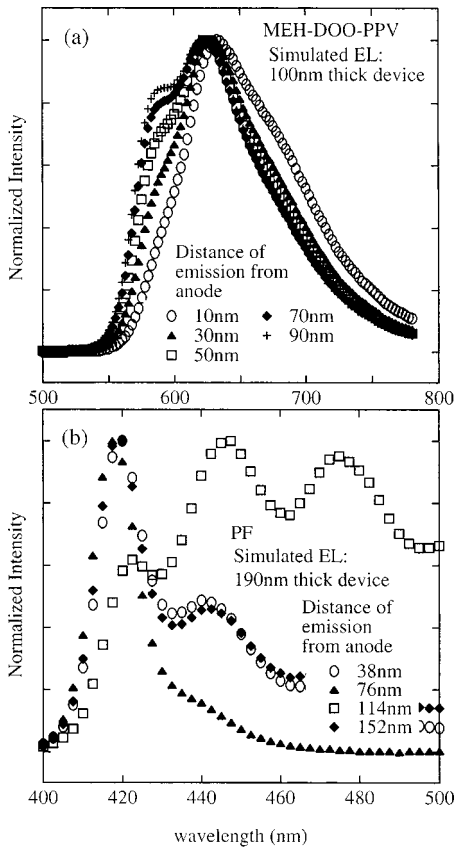

FIG. 6. Simulated normalized EL spectra for single device thickness as a function of emission zone for (a) 100 nm MEH-DOO-PPV device, with emission occurring at 10, 30, 70, and 90 nm from anode, and (b) 190 nm PF device, with emission occurring at 38, 76, 114, and 152 nm from anode.

Figure 7 shows the thickness dependent simulations recalculated under the assumption that the emission is occurring nearer to the cathode. In Fig. 7(a), the MEH-DOO-PPV simulation is done assuming emission to be a distance 70% of the emissive layer thickness away from the anode. In this case, the thickness-dependent trend seen in the experimental data is reproduced; however, the effect in simulation is less dramatic than seen in the experimental data. In Fig. 7(b), the PF simulation is done assuming emission to be a distance 80% of the emissive layer thickness away from the anode. Clearly in this case the thickness-dependent trend seen in the experimental data is no longer accurately reproduced. The emission location parameter used in the simulations of thick-

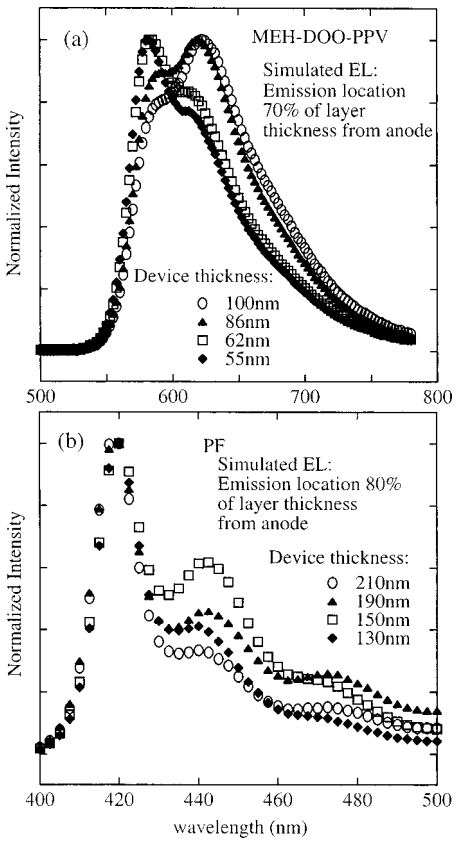

FIG. 7. Simulated normalized EL spectra for (a) MEH-DOO-PPV, with thicknesses 55, 62, 86, and 100 nm and emission assumed to occur 70% of device thickness away from the anode, and (b) PF, with thicknesses 130, 150, 190, and 210 nm, and emission assumed to occur 80% of device thickness away from the anode.

ness dependence in MEH-DOO-PPV and in PF devices were chosen such that the resulting simulated spectra and radiance trends most closely matched those seen in our experimental results. For both materials this value is 20% of the polymer layer thickness from the anode.

Finally, we consider whether recombination near the anode is consistent with our understanding of the device architecture. For PF, electron injection from the calcium cathode (work function $\Phi \sim 2.9$ eV) to the LUMO of PF (3.0 eV) is nearly Ohmic; however, a large barrier to hole injection exists from the PEDOT-PSS (5.1 eV) to the HOMO of PF (5.8 eV).[22] For PF without endcaps, it is thought by some that this barrier to hole injection causes electron-hole recombination to occur directly at the polymer/PEDOT-PSS interface. The endcaps appear to assist in hole injection into PF,[23] moving recombination slightly into the bulk of the material, increasing device efficiency and decreasing aggregation peaks associated with the polymer morphology at the interface.[24] It is therefore reasonable to assume in this scheme that recombination should occur near to the device anode, and light emission occurring at 20% of the polymer layer thickness from the anode would then be consistent with this assumption. However, there has been some evidence[25] that the lower electron mobility in PF's inhibits movement of electrons through the film toward the anode significantly enough that despite a barrier to hole injection at the interface, recombination may be occurring nearly at the cathode. In this scheme then, our assumptions are no longer accurate, and therefore our simulations do not provide a close match to experiment. In the case of PF materials, a straightforward conclusion about the location of recombination may not be possible based on injection barrier and mobility arguments alone.

In contrast, for MEH-PPV-DOO, both the HOMO (5.3 eV) and LUMO (3.0 eV) levels are closely matched to the electrodes,[26,27] providing nearly Ohmic contacts for both electron and hole injection. As a consequence, we would expect to see emission occurring at a thickness consistent with experimentally determined relative charge mobilities in the material. Due to its similarities with MEH-PPV, the hole mobilities for MEH-DOO-PPV should be on the order of, or slightly higher than, the electron mobilities.[28] This would suggest that recombination should occur close to the center or cathode side of the device rather than near to the anode.[29] However, the simulations of thickness dependence in MEH-DOO-PPV show rather low emission zone location sensitivity, and it is while it may not be the closest match to experiment, a simulation using an emission zone located closer to the cathode would still provide a reasonable simulation of MEH-DOO-PPV device thickness dependence.

VI. CONCLUSIONS

Several aspects of the simulations make it rather difficult to exactly reproduce the experimental data. As previously mentioned, the choice of dipole emission spectrum can significantly alter the overall appearance of the simulated spectra. In addition, the simulation can be rather sensitive to parameters that are experimentally determined, such as the thickness of both the hole injection layer and the polymer layer, and are therefore subject to experimental errors in comparing with experiment. Finally, assumptions are made in the calculations concerning the nature of charge recombination, exciton diffusion, and emission zone location which are not fully understood but which can change the final simulated thickness-dependent effects. We note that in polymer LED's as discussed here, the emission zone may extend over a few tens of nanometers. Thus the above model with an exact dipole location is an approximation.[30] However, the simulations are able to illustrate that the changes in the optical properties of polymer LED's seen as a function of device thickness can be well accounted for by simulation of optical interference effects.

ACKNOWLEDGMENTS

We would like to thank Yuko Nakazawa and Melissa Kreger for fruitful discussions. J.L. acknowledges support from the GAANN foundation. This work was supported by the National Science Foundation ECS-grant number 22201-443834.

*Author to whom correspondence should be addressed. Electronic mail: sacarter@cats.ucsc.edu

†Present address: Center for Computational Physics, Zurich University of Applied Science, 8401 Winterhur, Switzerland.

‡H.N. and U.S provided the PF materials for this work, and H.T. and H.H. provided the MEH-DOO-PPV used for this work.

[1] J. H. Burroughes, D. D. C. Bradley, A. R. Brown, R. N. Marks, K. Mackay, R. H. Friend, P. L. Burns, and A. B. Holmes, Nature (London) **347**, 539 (1990).

[2] R. H. Friend, R. W. Gymer, A. B. Holmes, J. H. Burroughes, R. N. Marks, C. Taliani, D. D. C. Bradley, D. A. Dos Santos, J. L. Bredas, M. Logdlund, and W. R. Salaneck, Nature (London) **397**, 121 (1999).

[3] D. Braun and A. J. Heeger, Appl. Phys. Lett. **58**, 1982 (1991).

[4] T.-Q. Nguyen, V. Doan, and B. J. Schwartz, J. Chem. Phys. **110**, 4068 (1999).

[5] M. Ariu, D. G. Lidzey, and D. D. C. Bradley, Synth. Met. **111–112**, 607 (2000).

[6] V. Cimrova and D. Neher, J. Appl. Phys. **79**, 3299 (1996).

[7] V. Bulovic, V. B. Khalfin, G. Gu, and P. E. Burrows, Phys. Rev. B **58**, 3730 (1998).

[8] H.-H. Hörhold, H. Tillmann, C. Bader, R. Stockmann, J. Nowotny, E. Klemm, W. Holzer, and A. Penzkofer, Synth. Met. **119**, 199 (2001).

[9] H. G. Nothofer, Ph.D. thesis, University of Potsdam, Potsdam, Germany.

[10] This is expected, due to the minimal optical interference present in a multilayered structure of very low variation in reflectivity. The geometry of the experimental apparatus is such that self-absorption effects are minimized.

[11] PEDOT-PSS-PSS is provided by Bayer Corporations.

[12] S. A. Carter, M. Angelopoulos, S. Karg, P. J. Brock, and J. C. Scott, Appl. Phys. Lett. **70**, 2067 (1997).

[13] R. Jakubiak, C. J. Collison, W. C. Wan, L. J. Rothberg, and B. R. Hsieh, J. Phys. Chem. A **103**, 2394 (1999).

[14] John Lekner, *Theory of Reflection* (Dodrecht, Nijhoff, 1987).

[15] G. Björk, S. Machida, Y. Yamamoto, and K. Igeta, Phys. Rev. A **44**, 669 (1991).

[16] O. H. Crawford, J. Chem. Phys. **89**, 6017 (1988).

[17] W. Lukosz, J. Opt. Soc. Am. **71**, 744 (1981).

[18] K. A. Neyts, J. Opt. Soc. Am. A **15**, 962 (1998).

[19] S. E. Burns, N. C. Greenham, and R. H. Friend, Synth. Met. **76**, 205 (1996).

[20] J.-S. Kim, P. K. H. Ho, N. C. Greenham, and R. H. Friend, J. Appl. Phys. **88**, 1073 (2000).

[21] L. A. A. Petterson, F. Carlsson, O. Inganas, and H. Arwin, Thin Solid Films **313**, 356 (1998).

[22] S. Janietz, D. D. C. Bradley, M. Grell, C. Giebeler, M. Inbasekran, and E. P. Woo, Appl. Phys. Lett. **73**, 2453 (1998).

[23] T. Miteva, A. Meisel, W. Knoll, H. G. Nothofer, U. Scherf, D. C. Müller, K. Meerholz, A. Yasuda, and D. Neher, Adv. Mater. **13**, 565 (2001).

[24] Y. K. Nakazawa, S. A. Carter, H.-G. Nothofer, U. Scherf, V. Y. Lee, R. D. Miller, and J. C. Scott, Appl. Phys. Lett. **80**, 3832 (2002).

[25] A. J. Campbell, H. Antoniadis, T. Virgili, D. G. Lidzey, X. Wang, and D. D. C. Bradley, Proc. SPIE **4464** (2002).

[26] Values given are those corresponding to the closely related materials PFO and MEH-PPV. We expect the true values to be very similar to those reported.

[27] I. H. Campbell, T. W. Hagler, D. L. Smith, and J. P. Ferraris, Phys. Rev. Lett. **76**, 1900 (1996).

[28] L. Bozano, S. A. Carter, J. C. Scott, G. G. Malliaras, and P. J. Brock, Appl. Phys. Lett. **74**, 1132 (1999).

[29] G. G. Malliaras and J. C. Scott, J. Appl. Phys. **83**, 5399 (1998).

[30] W. M. V. Wan, N. C. Greenham, and R. H. Friend, J. Appl. Phys. **87**, 2542 (2000).